Precision GeoSurveys

AIRBORNE GEOPHYSICAL SURVEY REPORT

Tosh

Burwash Landing, Yukon

Snowline Gold Corp.

Precision GeoSurveys Inc.

BC Permit to Practice 1002615

www.precisiongeosurveys.com

Hangar 42 Langley Airport

21330 - 56th Ave., Langley, BC

Canada V2Y 0E5

604-484-9402

Jen D. Hanlon, M.Sc., P.Geo.

August 2022

Job# 22149

Table of Contents

List of Figures

List of Tables

List of Appendices

List of Tosh Survey Block Plates

1.0 Introduction

This report describes the high-resolution helicopter-borne magnetic and radiometric survey completed by Precision GeoSurveys Inc. at the Tosh survey area for Snowline Gold Corp. The Tosh survey area is in southwestern Yukon (Figure 1) and the survey was flown from July 3 to July 6, 2022.

Figure 1: Tosh survey area located in southwestern Yukon.

1.1 Survey Area

The survey block is centered approximately 56 km northwest of Burwash Landing, Yukon (Figure 2).

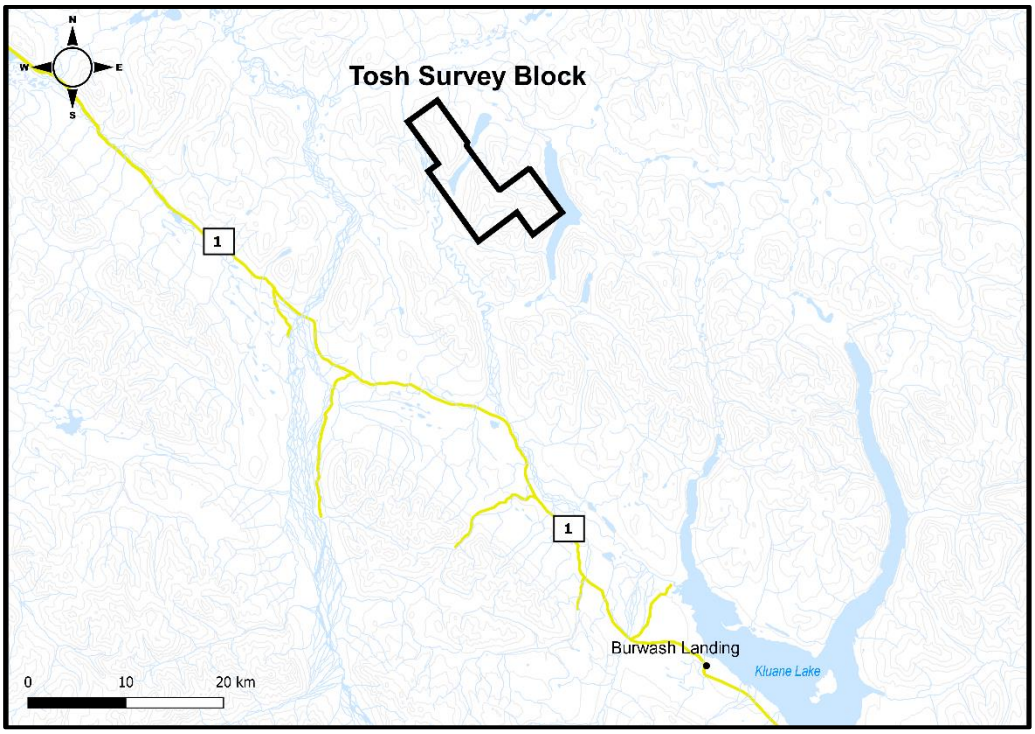

Figure 2: Tosh survey block 56 km northwest of Burwash Landing, Yukon.

The Tosh survey lines were flown at 100 m line spacing on a heading of 053°/233°, while tie lines were flown at 1000 m line spacing on a heading of 143°/323° (Figures 3 and 4).

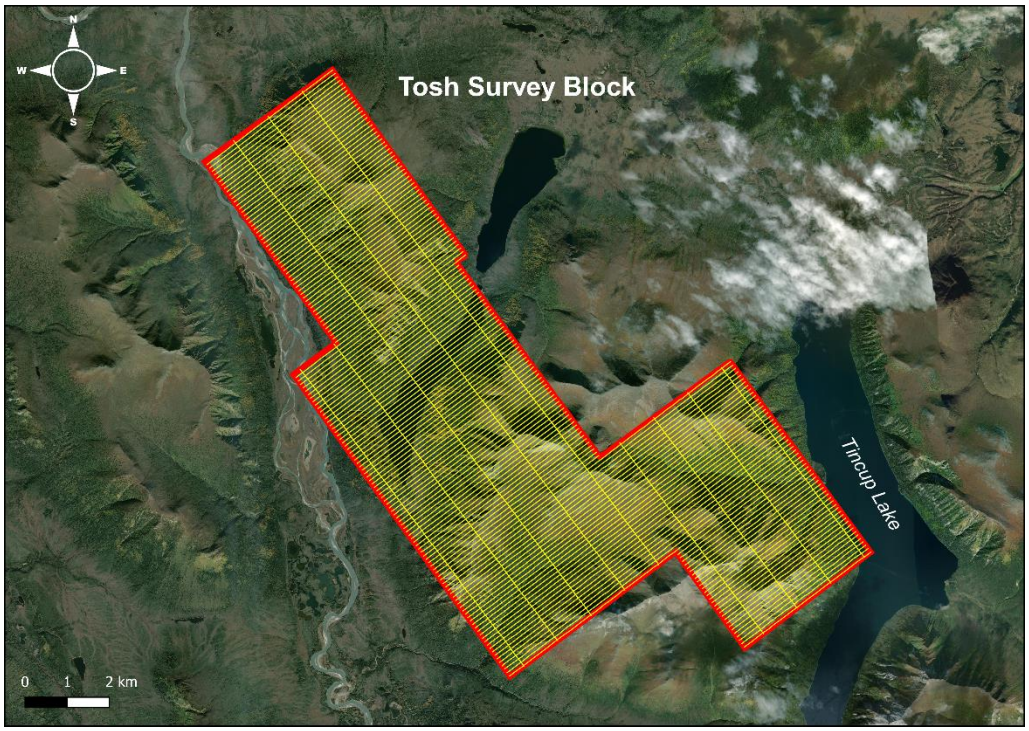

Figure 3: Plan View – Tosh survey block with actual flight lines in yellow and survey block boundary in red.

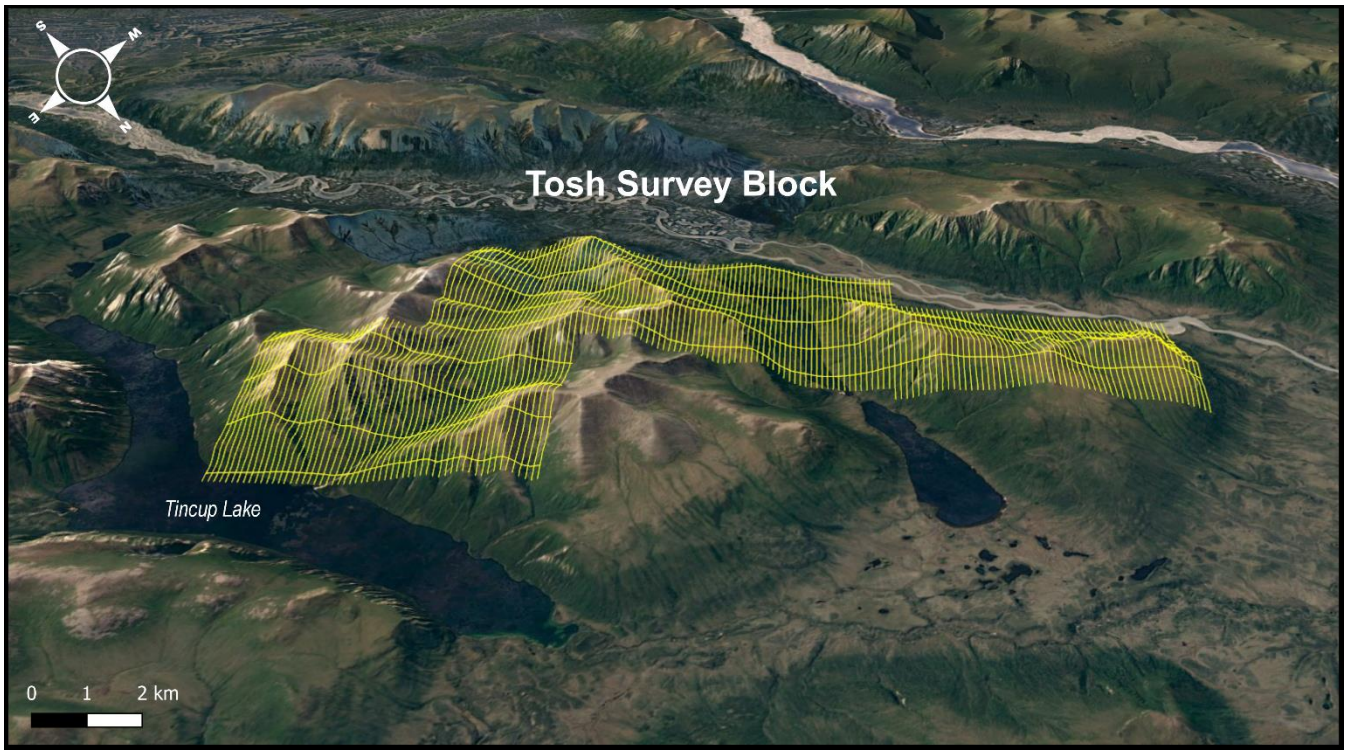

Figure 4: Terrain View – Tosh survey block with actual flight lines in yellow.

1.2 Survey Specifications

The geodetic system used for the geophysical survey was WGS 84 in UTM Zone 7N. A total of 913 line km was flown over an area of 82.8 km^2 (Table 1). Polygon coordinates for the Tosh survey block are specified in Appendix A.

Survey Block	Area (km^2)	Line Type	Line Orientation (UTM grid)	Line Spacing (m)	No. of Lines Planned	No. of Lines Completed	Total Planned Line km	Total Actual km Flown
Tosh	82.8	Survey	053°/233°	100	169	169	831	831
		Tie	143°/323°	1000	9	9	82	82
		Total:			**178**	**178**	**913**	**913**

Table 1: Survey flight line specifications for Tosh survey block.

2.0 Geophysical Data

Geophysical data are collected in a variety of ways and are used for many purposes including aiding in the determination of geology, mineral deposits, oil and gas deposits, geotechnical investigations, contaminated land sites, and UXO (unexploded ordnance) detection.

For the purposes of this survey, airborne magnetic and radiometric data were collected to serve in geological mapping and exploration for mineral deposits.

2.1 Magnetic Data

Magnetic surveying is the most common airborne geophysical technology used for both mineral and hydrocarbon exploration. Aeromagnetic surveys record the intensity of the total magnetic field measured at a magnetometer sensor, which is fixed to the aircraft. The total magnetic field is comprised of the desired geomagnetic field in combination with undesired influences from varying solar wind and the aircraft's inherent magnetic field. Subtracting the undesired magnetic effects from the total field results in aeromagnetic maps that show the spatial distribution and relative abundance of magnetic minerals - most commonly the iron oxide mineral magnetite - in the upper levels of Earth's crust. These results, in turn, can then be related to geological attributes such as lithology, structure, and alteration of bedrock. Survey specifications, instrumentation, and interpretation procedures depend on the individual objectives of each survey. Magnetic surveys are typically performed for:

- Geological Mapping - to aid in mapping lithology, structure, and alteration.
- Identification of variations in ferromagnetic response directly or indirectly related to mineral deposits.
- Depth to Basement Mapping - for exploration in sedimentary basins or mineralization associated with the basement surface.

2.2 Radiometric Data

Radiometric surveys are used to determine the absolute or relative concentrations, or both, of the naturally occurring radioelements uranium (U), thorium (Th), and potassium (K) in surface rocks and soils using radioactive emanations. Mapping the distribution and concentration of radioelements is useful for:

- Determining different lithologies based on characteristic radioelement geochemistry, either absolute or relative. For example, natural radioactivity of igneous rocks generally increases with SiO_2 content.
- Identification of hydrothermal alteration. For example, individual radioelements follow very different pathways of evolution during alteration of rocks, particularly potassic enrichments.
- Exploration for valuable mineral deposits related to increases in radioelement concentrations such as uranium and rare earth elements.
- Providing insights into weathering. For example, clay minerals tend to fix the natural radioelements in near-surface environments.
- Environmental mapping purposes, such as delineation of surface drainage features.

Gamma rays are electromagnetic waves with frequencies between 10^{19} and 10^{21} Hz emitted spontaneously from an atomic nucleus during radioactive decay, in packets referred to as photons. The energy E transported by a photon is related to the wavelength λ or frequency ν by the formula:

$$E = h\nu = hc/\lambda$$

where: c is the velocity of light
h is Planck's constant (6.626×10^{-34} joule)

All detectable gamma radiation from Earth materials comes from the natural decay products of three primary radioelements: U, Th, and K. Each individual nuclear species (element) emits gamma rays at one or more specific energies, as shown in Figure 5. Of these elements, only potassium (^{40}K) emits gamma energy directly, at 1.46 MeV. Uranium (^{238}U) and thorium (^{232}Th) emit gamma rays through their respective decay series; ^{214}Bi at 1.76 MeV for uranium and ^{208}Tl at 2.61 MeV for thorium. Accordingly, the ^{214}Bi and ^{208}Tl measurements are considered equivalents for uranium (eU) and thorium (eTh), as the daughter products will be in equilibrium under most natural conditions.

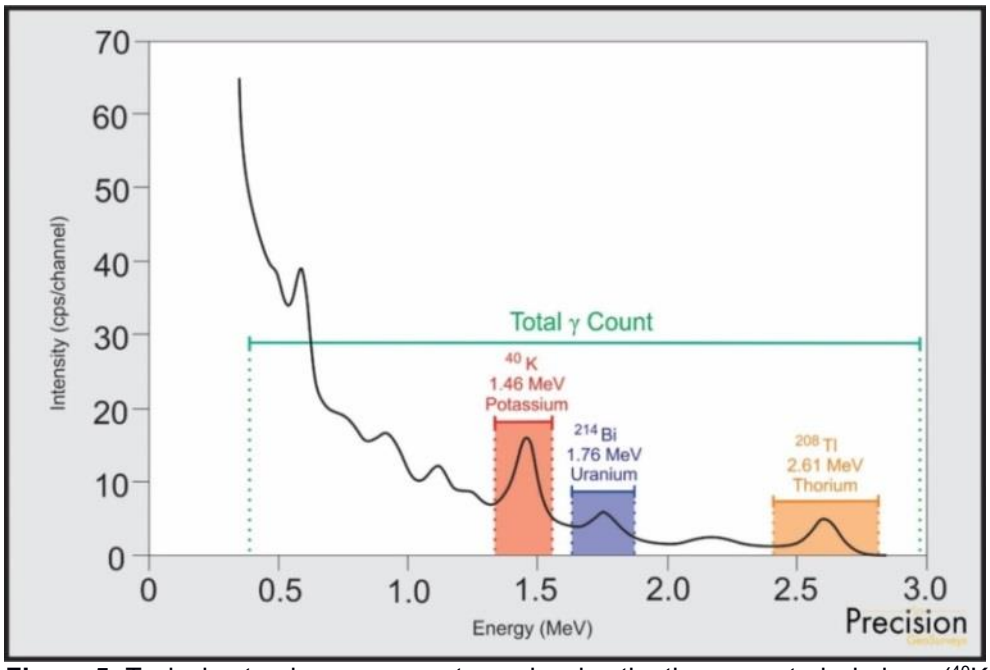

Figure 5: Typical natural gamma spectrum showing the three spectral windows (^{40}K 1.37-1.57 MeV, ^{214}Bi 1.66-1.86 MeV, ^{208}Tl 2.41-2.81 MeV) and total count (0.40-2.81 MeV) window.

Surficial debris, vegetation, standing water (lakes, marshes, swamps), ice, and snow can attenuate gamma rays originating from the underlying rocks. Therefore, surficial conditions must be evaluated before attributing variations in gamma counts to changes in the underlying geology. An increase in soil moisture can also significantly affect gamma radiation concentrations. For example, a 10% increase in soil moisture can decrease the measured gamma radiation by about

the same amount. Radon isotopes are long-lived members of both the U and Th decay series and Ra mobility can influence radiometric surveys. In addition to being directly radioactive, ^{226}Ra and ^{222}Rn can attach to dust particles in the atmosphere. Precipitation of these radioactive dust particles by rain can lead to apparent increases of more than 2000% in uranium ground concentration (IAEA, 2003). Therefore, gamma data are not typically collected during a rainfall, or shortly after a rainfall.

3.0 Aircraft and Equipment

All geophysical and subsidiary equipment were carefully installed on an aircraft by Precision GeoSurveys to collect magnetic and radiometric data.

3.1 Aircraft

Precision GeoSurveys flew the survey using an Airbus AS350 helicopter, registration C-GOHK.

3.2 Geophysical Equipment

The survey aircraft (Figure 6) was equipped with a data acquisition system, GPS navigation system, pilot guidance unit (PGU), laser altimeter, cesium vapor magnetometer, fluxgate magnetometer, gamma ray spectrometer, barometer, and temperature/humidity probe. In addition, a magnetic base station was used to record temporal magnetic variations. Technical specifications for the geophysical equipment are provided in Appendix B.

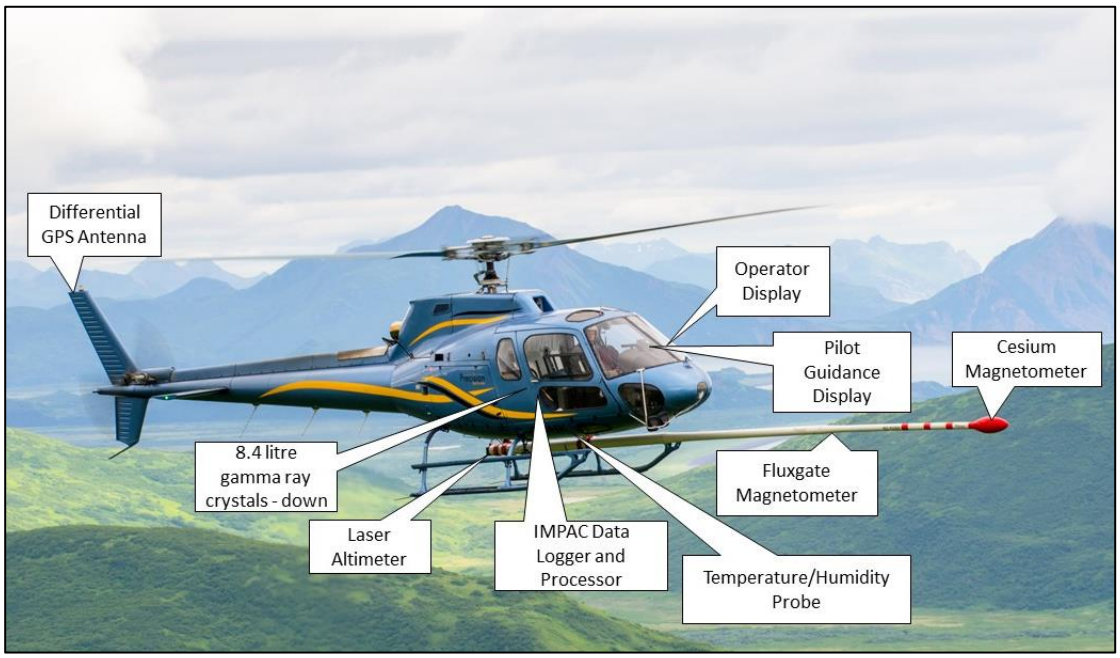

Figure 6: Survey helicopter equipped with a magnetic sensor for magnetic data acquisition and gamma ray spectrometer for radiometric measurements.

3.2.1 IMPAC

The Integrated Multi-Parameter Acquisition Console (IMPAC) (Figure 7), manufactured by Nuvia Dynamics Inc. (previously Pico Envirotec Inc.), is the main computer used in integrated data recording, data synchronizing, providing real-time quality control data for the geophysical operator display, and the generation of navigation information for the pilot and operator display systems.

Figure 7: IMPAC data acquisition system.

IMPAC uses the Microsoft Windows operating system and geophysical parameters are based on Nuvia's Airborne Geophysical Information System (AGIS) software. Depending on survey specifications, information such as magnetic field, electromagnetic response, total gamma count, counts of various radioelements (K, U, Th, etc.), cosmic radiation, barometric pressure, atmospheric humidity, temperature, aircraft attitude, aircraft height, navigation parameters, and GPS status can all be monitored on the AGIS on-board display (Figure 8).

While in flight, the raw magnetic response, magnetic fourth difference, compensated and uncompensated data, radiometric spectra, aircraft position, survey altitude, cross track error, and other parameters are recorded (depending on sensor configuration) and can be viewed by the geophysical operator for immediate quality control (QC). Additional software allows for post or real time magnetic compensation.

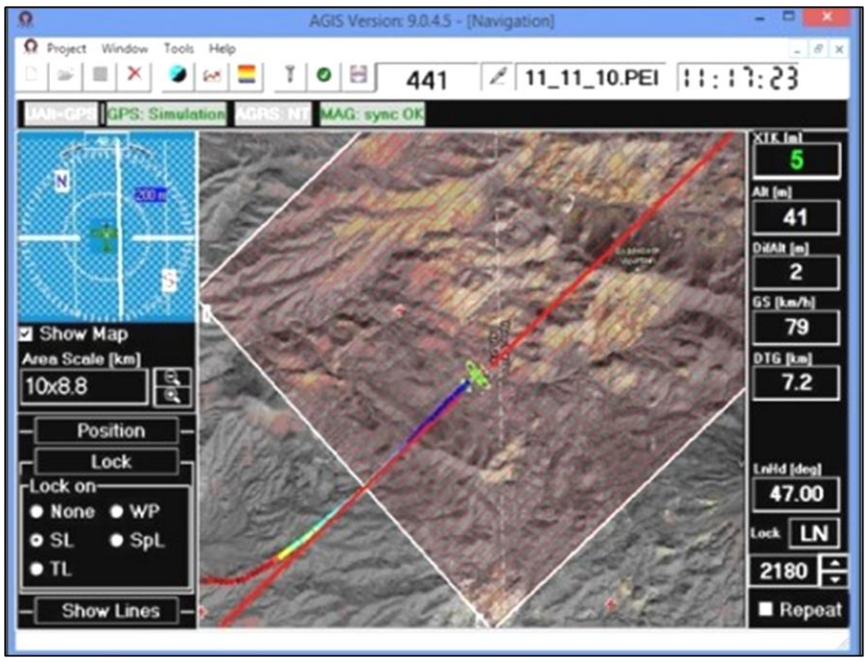

Figure 8: AGIS operator display showing real time flight line recording and navigation parameters. Additional windows display real-time geophysical data to operator.

3.2.2 GPS Navigation System

A Hemisphere R330 GPS receiver (Figure 9) and a Novatel GPS antenna on the tail of the aircraft integrated with the AGIS navigation system and pilot display (PGU) provide accurate navigational information and position control. The R330 GPS receiver supports fast updates at a rate of up to 10 Hz (10 times per second), delivering sub-meter positioning accuracy in three dimensions. It receives GNSS (GPS/GLONASS) L1 and L2 signals.

Differential correction methods including WAAS, L-Band, RTK, SBAS, and Beacon are supported by the R330. Innovative Hemisphere GPS Eclipse SureTrack technology allows the receiver to model the phase on satellites that the airborne unit is currently tracking. With SureTrack technology, dropouts are reduced and speed of the signal reacquisitions is increased, which enhances accurate positioning when base corrections are temporarily not available.

Figure 9: Hemisphere R330 GPS receiver.

3.2.3 Pilot Guidance Unit

Steering and elevation (ground clearance) information is continuously provided to the pilot by the Pilot Guidance Unit (PGU). The graphical display is mounted on top of the aircraft's instrument panel, remotely from the data acquisition system. The PGU is the primary navigation aid (Figure 10) to assist the pilot in keeping the aircraft on the planned flight path, heading, speed, and at the desired ground clearance.

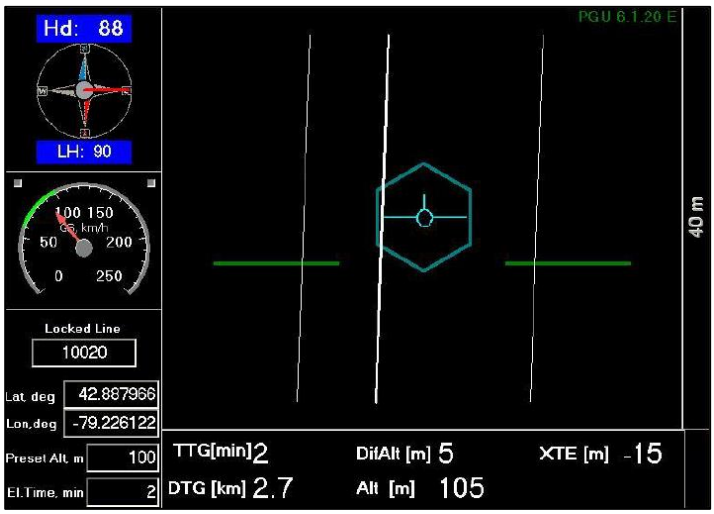

Figure 10: PGU screen displaying navigation information.

PGU information is displayed on a full VGA 600 x 800-pixel 7-inch (17.8 cm) LCD display. The CPU for the PGU is contained in a PC-104 console and uses Microsoft Windows operating system control, with input from the GPS antenna on the aircraft, laser altimeter, and AGIS.

3.2.4 Laser Altimeter

Terrain clearance is measured by an Opti-Logic RS800 Rangefinder laser altimeter (Figure 11) attached to the aft end of the magnetometer boom. The RS800 laser is a time-of-flight sensor that measures distance by a rapidly modulated and collimated laser beam that creates a dot on the target surface. The maximum range of the laser altimeter is 700 m off natural surfaces with accuracy of ±1 m on a 1 x 1 m diffuse target with 50% (±20%) reflectivity. Within the sensor unit, reflected signal light is collected by the lens and focused onto a photodiode. Through serial communications and digital outputs, ground clearance data are transmitted to an RS-232 compatible port and recorded and displayed by the AGIS and PGU at 10 Hz in meters.

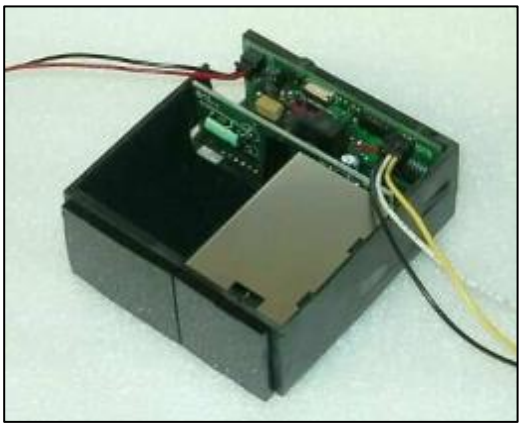

Figure 11: Opti-Logic RS800 Rangefinder laser altimeter.

3.2.5 Magnetometer

The survey was flown with a Scintrex CS-3 split-beam cesium vapor magnetometer (Figure 12) mounted on the front of the helicopter in a non-magnetic and non-conductive "stinger" configuration to measure total magnetic intensity. The magnetometer sensor was oriented at 45° to couple with local magnetic field at the Tosh survey area.

Figure 12: Scintrex CS-3 cesium vapor magnetometer.

3.2.6 Fluxgate Magnetometer

As the survey helicopter flies along a survey line, small attitude changes (pitch, roll, and yaw) are measured by a triaxial fluxgate magnetometer (Figure 13). The fluxgate consists of three magnetic sensors, X, Y, and Z, operating independently and simultaneously. Each sensor has an analog output corresponding to the directional component of the ambient magnetic field along its axis. Response of the sensors is proportional to the cosine of the angle between the applied field and the sensor's sensitive axis.

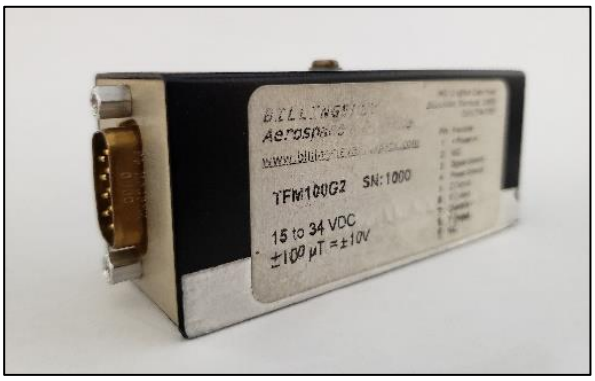

Figure 13: Billingsley TFM100G2 triaxial fluxgate magnetometer.

3.2.7 Magnetic Base Station

Temporal variations of Earth's magnetic field were monitored and recorded by a GEM GSM-19T base station magnetometer. It was operated at all times during surveying. The base station was located in an area with low magnetic gradient (i.e., away from electric power transmission lines and moving ferrous objects, such as motor vehicles), for optimum survey data integrity.

The GEM GSM-19T magnetometers (Figure 14) with integrated GPS time synchronization uses proton precession technology with absolute accuracy of ±0.20 nT and sensitivity of 0.15 nT at 1 Hz. Base station magnetic data were recorded on internal solid-state memory and downloaded onto a field laptop using a serial cable and GEMLink 5.4 software. Profile plots of the base station readings were generated, updated, and reviewed at the end of each survey day.

Figure 14: GEM GSM-19T proton precession magnetometer.

3.2.8 Spectrometer

Gamma radiation data were collected by an Advanced Gamma Ray Spectrometer (AGRS-2) manufactured by Nuvia Dynamics. The AGRS-2 is an intelligent, self-calibrating, fully integrated gamma detection system (Figure 15) containing two thallium-activated synthetic sodium iodide crystals: 8.4 litres (two crystals of 4.2 liters each) downward-looking, with user-selectable 256, 512, or 1024 channel output at 1 Hz sampling rate. The downward-looking crystals are designed to measure gamma rays from below the aircraft. The AGRS-2 system is installed in the rear passenger cabin of the helicopter away from the fuel tank to minimize variable gamma attenuation from fluctuating fuel levels.

Figure 15: AGRS-2 gamma spectrometer system with two downward detectors; 8.4 litres in total.

4.0 Survey Operations

The Tosh geophysical survey was flown from July 3 to July 6, 2022 in summer conditions. The experience of the pilot ensured that data quality objectives were met, and the safety of the flight crew was never compromised given the potential risks involved in airborne geophysical surveying. Field processing and quality control checks were performed daily.

4.1 Operations Base and Crew

The base of operation for the Tosh survey was at the Burwash Landing, Yukon, 56 km southeast of the survey block.

Precision's geophysical crew consisted of five members (Table 2):

Crew Member	Position
Harmen Keyser, P.Geo.	Helicopter pilot
Puraz Shirzad, B.A.	GIS technician – mapping (off-site)
Jenny Poon, B.Sc., P.Geo.	Geophysicist – data processor (off-site)
Shawn Walker, M.Sc., P.Geo.	Geophysicist – data processor (off-site) and project manager
Jen Hanlon, M.Sc., P.Geo.	Geophysicist – Reporting (off-site)

Table 2: List of survey crew members.

4.2 Magnetic Base Station Specifications

Changes in Earth's magnetic field over time, such as diurnal variations, magnetic pulsations, and geomagnetic storms, were measured and recorded by a stationary GEM GSM-19T proton precession magnetometer. The magnetic base station was installed on a ridge within the survey area (Table 3; Figures 16 and 17) in an area away from sources of potential interference such as ferromagnetic objects, vehicles, and power lines that could affect the base station data and ultimately the survey data.

Station Name	Easting/Northing	Latitude/Longitude	Datum/Projection
GEM 3 S/N 5081669	586647 m E 6851285 m N	61° 47' 04.74" N 139° 21' 25.82" W	WGS 84, Zone 7N

Table 3: Magnetic base station location.

Magnetic readings were reviewed at regular intervals to ensure that no airborne data were collected during periods of high magnetic activity (i.e., in excess of 10 nT from a linear chord length of five minutes).

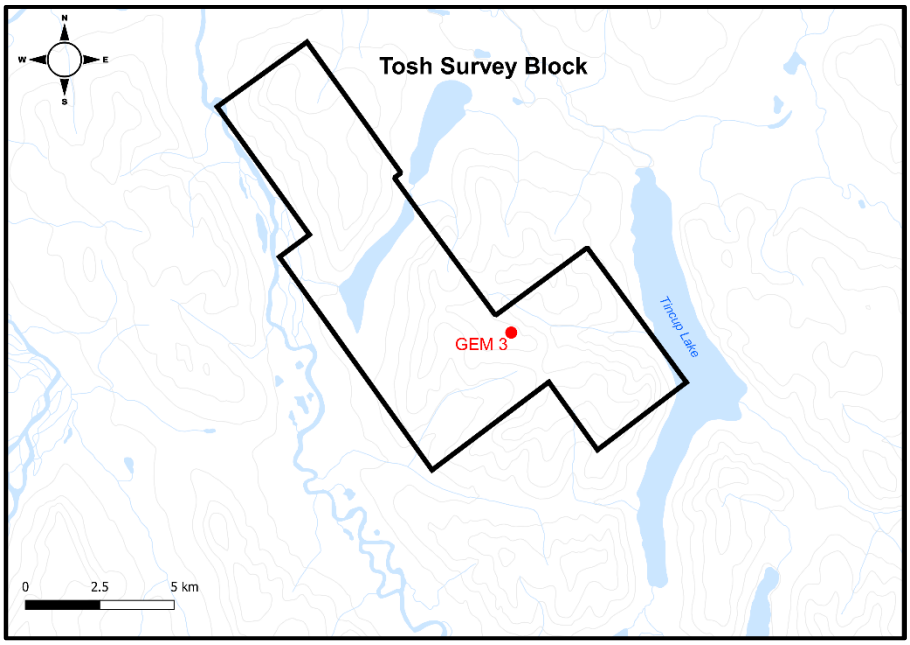

Figure 16: Location of GEM 3 magnetic base station within the Tosh survey area.

Figure 17: GEM 3 magnetic base station.

4.3 Field Processing and Quality Control

Survey data were transferred from the aircraft's data acquisition system onto a USB memory stick and copied onto a field data processing laptop on a flight-by-flight basis. The raw data files in PEI binary data format were converted into Geosoft GDB database format. Using Geosoft Oasis Montaj 2021.2.1.11, the data were inspected to ensure compliance with contract specifications (Table 4; Figures 18 to 20).

Parameter	Specification	Tolerance
Position	Line Spacing	Flight line deviation within 8 m L/R from ideal flight path. No exceedance for more than 1 km.
	Height	Nominal flight height of 50 m above ground level (AGL) with tolerance of ±10 m. No exceedance for more than 1 km, provided deviation is not due to tall trees, topography, mitigation of wildlife/livestock harassment, cultural features, or other obstacles beyond the pilot's control.
	GPS	GPS signals from four or more satellites must be received at all times, except where signal loss is due to topography. No exceedance for more than 1 km.
Magnetics	Temporal/Diurnal Variations	Non-linear temporal magnetic variations within 10 nT of a linear chord of 5 minutes length.
	Normalized 4th Difference	Magnetic data within 0.02 nT peak to peak. No exceedance for distances greater than 1 km or more, provided noise is not due to geological or cultural features.
Radiometrics	Moisture Conditions	No delays shall be incurred due to unfavourable radiometric survey conditions.

Table 4: Contract survey specifications.

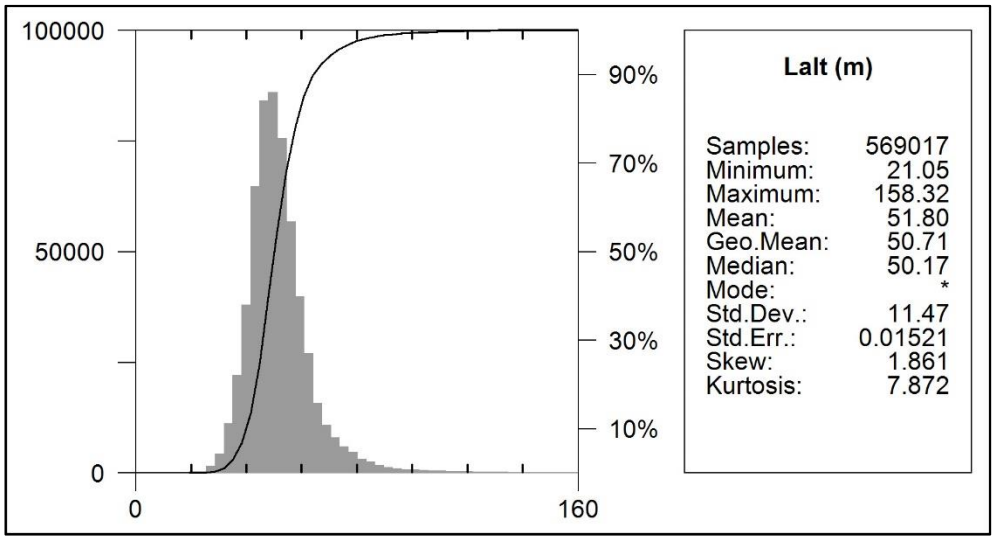

Figure 18: Histogram showing survey elevation vertically above ground.

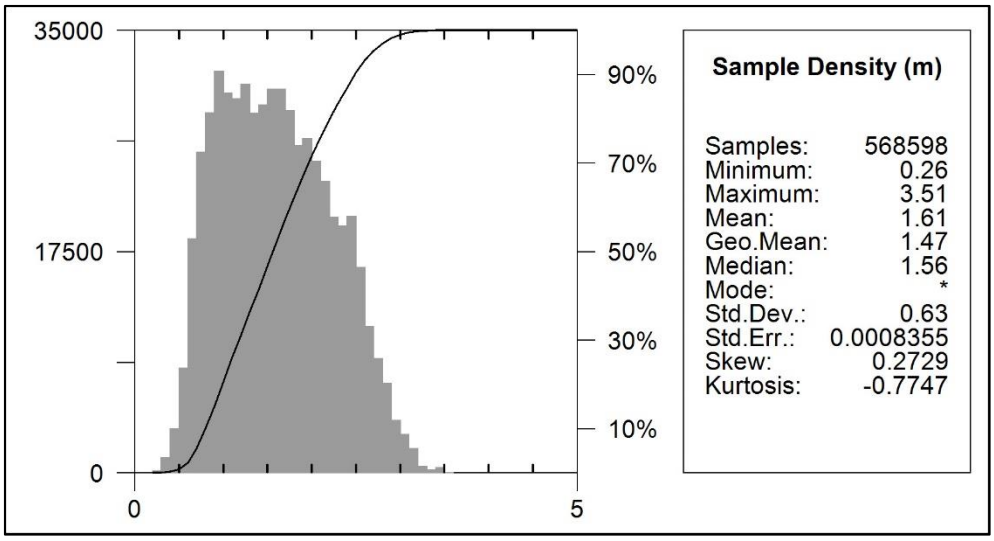

Figure 19: Histogram showing magnetic sample density. Horizontal distance in meters between adjacent measurement locations; magnetic sample frequency 20 Hz.

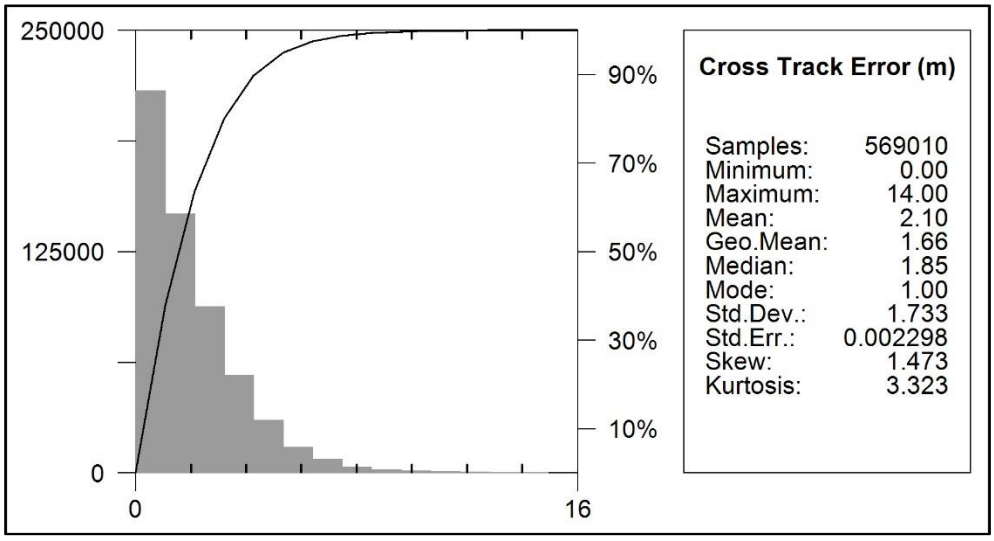

Figure 20: Histogram showing cross track error of survey helicopter.

5.0 Data Acquisition Equipment Checks

Equipment tests and calibrations were conducted for the laser altimeter, magnetometer, and spectrometer at the start of the survey to ensure compliance with contract specifications and to deliver high quality airborne geophysical data. A lag test was conducted for all sensors. For the airborne magnetometer compensation and heading error test flights were flown. There were three tests conducted for the gamma spectrometer: calibration pad test, cosmic flight test, and altitude correction and sensitivity test.

5.1 Laser Altimeter Calibration

The Opti-Logic RS800 laser altimeter used on the survey helicopter was tested and calibrated in accordance with manufacturer's instructions prior to starting the survey. This ensured that heights reported by the laser were accurate within the normal survey operating range.

5.2 Lag Test

A lag test was performed to determine the time difference between recording the digital readings from the magnetometer and laser altimeter, and the fiducially marked position fix time of the readings obtained by the GPS system. Lag can result from a combination of system lag and varying distances of the sensors with respect to the GPS antenna. The test was flown in reciprocal headings over identifiable features at survey speed and height to isolate position changes. The resulting data (Table 5) were used to correct for time and position.

Instrument	Source	Lag Fiducial	Correction (sec)
Magnetometer	Logging machinery	5	0.25
Laser	Sharp gully	16	0.80
Spectrometer	Lake edge	20	1.00

Table 5: Survey lag correction values. Magnetic data at 20 Hz; laser altimeter and spectrometer were resampled to 20 Hz.

5.3 Magnetometer Tests

The magnetometer was tested and calibrated with a series of dedicated flights specifically for removing instrument offset errors and undesired effects of aircraft movement, speed, and heading direction.

5.3.1 Compensation Flight Test

During aeromagnetic surveying, the magnetometer is located within the aircraft's magnetic field and are therefore influenced by changes in the aircraft attitude and permanent magnetization of ferrous aircraft components. To remove this noise, the aircraft was degaussed using proprietary technology prior to the survey and the remaining magnetic noise was removed by a process called magnetic compensation.

Magnetic compensation is achieved by completing a series of prescribed maneuvers in flight (±10° roll, ±10° pitch, and ±10° yaw) over each of the four orthogonal headings utilized within the survey area. The maneuvers must be completed at a sufficient altitude (typically > 2,500 m AGL) in an area of low magnetic gradient, so that Earth's magnetic field becomes nearly uniform at the altitude of the compensation flights. In each heading direction, three instances of the roll, pitch, and yaw maneuvers (total 36) are performed at constant elevation with the maneuvers recorded by the

fluxgate magnetometer relative to the ambient magnetic field. In this manner, the magnetic response at the airborne magnetometers can be attributed to aircraft movement, and the necessary parameters can be calculated to remove aircraft movement noise from the survey data. Compensation flight test results are summarized in Table 6.

Pre-Compensation (nT)					Post-Compensation (nT)				
Heading	**Roll**	**Pitch**	**Yaw**	**Total**	**Heading**	**Roll**	**Pitch**	**Yaw**	**Total**
053°	2.6238	0.8424	0.9407	4.4069	053°	0.1771	0.1565	0.1392	0.4728
143°	2.1340	0.9903	1.2319	4.3562	143°	0.0938	0.1152	0.1007	0.3097
233°	2.1006	1.7980	0.9849	4.8835	233°	0.1610	0.4982	0.3729	1.0321
323°	2.0721	0.8900	0.6649	3.6270	323°	0.2111	0.2551	0.2128	0.6790
Figure of Merit = 17.2736					**Figure of Merit = 2.4936**				

Table 6: Results of compensation flight.

5.3.2 Heading Correction Test

To determine heading errors, a cloverleaf pattern flight test was conducted at high altitude to minimize the effect of natural magnetic gradient. The cloverleaf test was flown in the same orthogonal headings as the survey and tie lines at >2500 m AGL in an area with low magnetic gradient. For all four directions of the cloverleaf test the survey helicopter must pass over the same point, at the same elevation, with the aircraft in straight and level flight. The difference in magnetic values obtained in reciprocal headings is referred to as the heading error. Heading correction values derived from the test flight are summarized in Table 7.

Heading	Heading Correction (nT)
053°	-6.27
143°	-6.14
233°	5.49
323°	6.92
Total:	**0.0000**

Table 7: Magnetic sensor heading corrections.

5.4 Gamma-ray Spectrometer Tests and Calibrations

Calibration and testing of the AGRS-2 airborne gamma-ray spectrometry system was carried out prior to starting the survey. Spectrometer calibration involved three tests which enabled the conversion of airborne data to ground concentration of natural radioactive elements. These tests were the calibration pad test, cosmic flight test, and the altitude correction and sensitivity test. Procedures were generally in accordance with IAEA technical report series No. 323, *Airborne Gamma Ray Spectrometer*

Surveying, and AGSO Record 1995/60, *A Guide to the Technical Specifications for Airborne Gamma-Ray Surveys*.

5.4.1 Calibration Pad Test

The calibration pad test was conducted using Geological Survey of Canada (GSC) portable calibration pads. The pads are slabs of concrete containing known concentrations of the natural radioelements K, Th, and U and are used to simulate ideal geological sources of radiation. The measurements collected from the calibration pad test were used to determine Compton scattering and Grasty backscatter (spectral overlap between element windows) coefficients.

5.4.2 Cosmic Flight Test

While the background source of gamma radiation from the aircraft itself is essentially constant, the amount of signal detected from ground sources varies with ground clearance. As the height of the aircraft increases, the distance between the ground and the spectrometer crystals increases, and the proportion of cosmic radiation in each spectral window increases exponentially. The cosmic flight test is conducted to determine the aircraft's background attenuation coefficients for the detector crystal packs and the cosmic coefficients. The pilot is required to fly over the same low gamma source location (such as a large lake) repeatedly at 4000, 5000, 6000, 7000, and 8000 feet (1220, 1520, 1830, 2130, and 2440 m) above ground, for approximately two minutes each, to collect gamma data used to determine the non-terrestrial component present in the total gamma signal.

5.4.3 Altitude Correction and Sensitivity Test

The altitude and sensitivity test is similar to the cosmic flight test but is conducted at lower elevations. The aircraft is required to fly over the same location at 30, 40, 50, 60, 70, 100, and 120 m above ground, for two minutes each. As the distance between the gamma detectors on the aircraft and the radioactive ground source increases, the source signature exponentially degrades. As a result, this test is used to determine the altitude attenuation coefficients and the radio-element sensitivity of the airborne spectrometer system.

6.0 Data Processing

After all data were collected, several procedures were undertaken to ensure that the data met a high standard of quality. Magnetic and radiometric data recorded by the IMPAC were converted into Geosoft or ASCII file formats using Nuvia Dynamics software. Further processing (Figure 21) was carried out using Geosoft Oasis Montaj 2021.2.1.11 geophysical processing software along with proprietary processing algorithms.

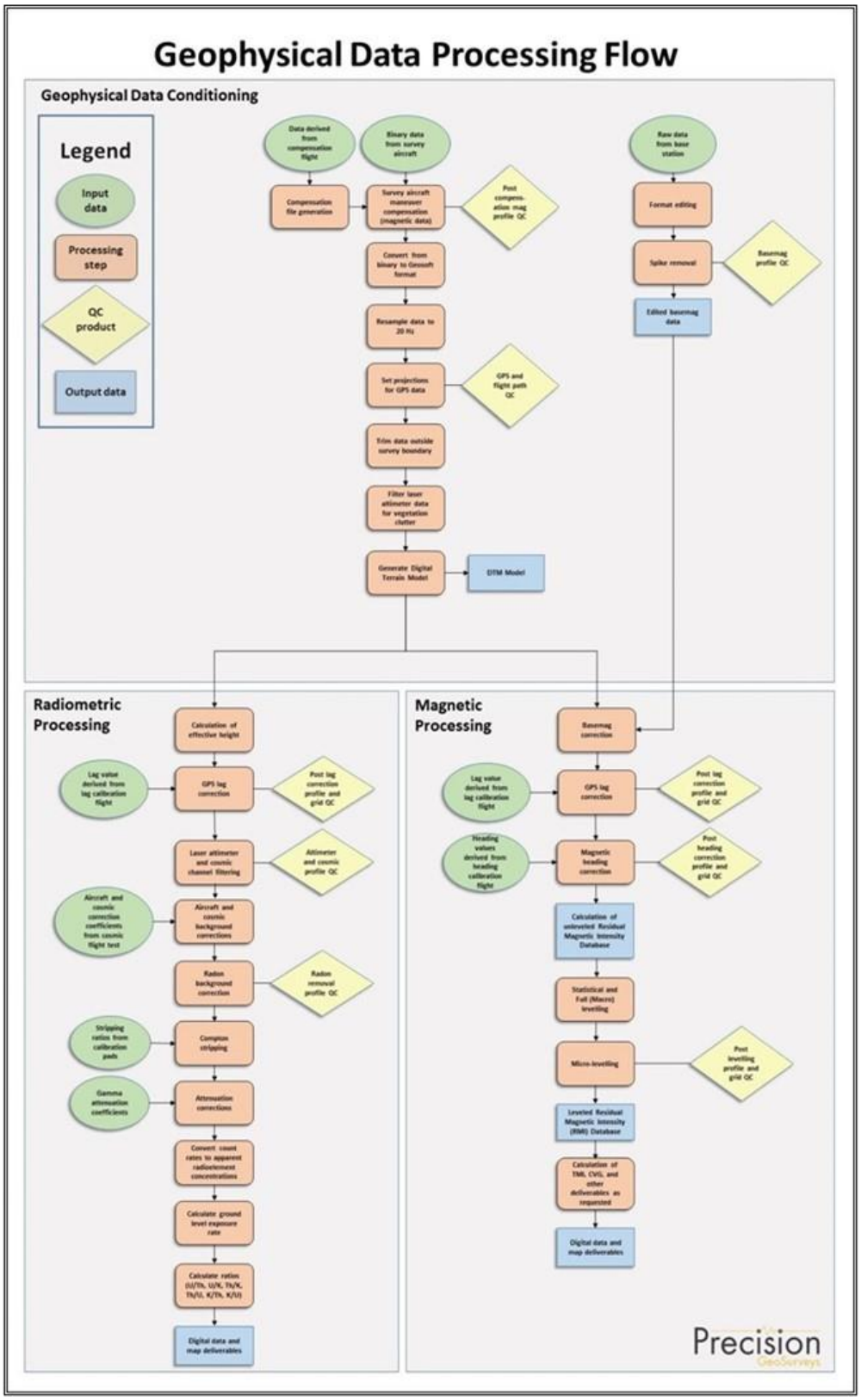

Figure 21: Magnetic and radiometric data processing flow.

6.1 Position Corrections

In order to collect high resolution geophysical data, the location at which the data were collected and recorded must be accurate.

6.1.1 Lag Correction

A correction for lag error was applied to the geophysical data recorded at each individual sensor to compensate for the lag caused by the distance between the GPS antenna, the recording system and the sensing instrument. Validity of the lag corrections was confirmed by the absence of grid corrugations in adjoining reciprocal lines.

6.2 Flight Height and Digital Terrain Model

Laser altimeters are unable to provide valid data over glassy water or fog which scatter the laser so that a "zero" reading is obtained. In these cases, estimates of correct height are inserted manually. Dense vegetation generates high frequency variations from leaf and branch reflections. A Rolling Statistics filter is applied to the lag corrected laser altimeter data to remove vegetation clutter followed by a Low Pass filter to smooth out the laser altimeter profile to eliminate isolated high frequency noise and generate a surface that closely corresponds to the actual ground profile.

As the GPS antenna is on the tail of the helicopter, altitude data were corrected by subtracting 3.1 m to place measured heights in the same plane as the laser altimeter. A Digital Terrain Model (DTM) was determined by subtracting the laser altimeter data from the filtered GPS altimeter data defined by the WGS 84 ellipsoidal height. DTM accuracy is affected by the attitude of the aircraft, slope of the ground, sample density, and satellite geometry. Small inconsistencies in recorded flight height at the intersection points of survey lines and tie lines resulted in small spatial variabilities in the Digital Terrain Model (DTM). Conventional leveling and micro-leveling were applied to correct for these variations and a fully leveled DTM was generated.

6.3 Magnetic Processing

Magnetic data were compensated and then corrected for temporal variations (including diurnal), lag, and heading. The data were examined for magnetic noise and spikes, which were removed as required. The background magnetic field, International Geomagnetic Reference Field (IGRF) of the Earth, was removed and survey and tie line data of the resulting residual magnetic field were then leveled.

6.3.1 Flight Compensation

Data obtained from the compensation flight test were applied to the raw magnetic data as the first step of data processing. A computer program called MAGComp was used to create a model from the compensation flight test for each survey to remove the noise induced by the aircraft and its movement; this model was applied to data from each survey flight.

6.3.2 Temporal Variation Correction

The intensity of Earth's magnetic field varies with position and time. The time variable, known as diurnal or more accurately as temporal variation, is removed from the recorded airborne data to provide the desired magnetic field at a specified position. Magnetic data from base station GEM 3 were used for correcting the airborne magnetic survey data. The data were edited, plotted, and merged into a Geosoft database (.GDB) on a daily basis.

Base station measurements were averaged to establish a magnetic reference datum of 56000.99 nT. Magnetic deviations relative to the reference datum were used to calculate the observed variations of the Earth's magnetic field during the time it took to complete the survey. The airborne magnetic data were then corrected for temporal variations by subtracting the base station deviations from the data collected on the aircraft.

6.3.3 Heading Correction

For each survey heading, changes in instrument magnetic fields along a survey flight line are detected and these systematic shifts are recorded. These values are used to construct a heading table (.TBL) file. An intersection table was created, containing all magnetic field values where tie lines intersected the survey lines, and the overall average magnetic field value was calculated. For each of the four headings, the averages were calculated and then compared to the overall average to determine four values which were used to correct heading and offset errors in each flight direction.

6.3.4 IGRF Removal

The International Geomagnetic Reference Field (IGRF) model is the empirical representation of Earth's dynamic magnetic field (main core field without external sources) collected and disseminated from satellite data and from magnetic observatories around the world. The IGRF has historically been revised and updated every five years by a group of modellers associated with the International Association of Geomagnetism and Aeronomy (IAGA).

The initial unleveled Residual Magnetic Intensity (RMI) was calculated by taking the difference between the 13th generation IGRF (IGRF-13, released in December 2019) and the non-leveled

Total Magnetic Intensity (TMI) to create a more valid model of individual near-surface magnetic anomalies. This model is independent of time to allow for other magnetic data (previous or future) to be more easily incorporated into each survey database.

6.3.5 Leveling and Micro-leveling

Small inconsistencies in flight height and line orientation result in small spatial variabilities in magnetic intensity measured at the intersection points of survey lines and tie lines. Using the initial Total Magnetic Intensity (TMI) data, data from survey and tie lines were leveled to each other. Two types of leveling were applied to the corrected data: conventional leveling and micro-leveling. There are two components to conventional leveling: statistical leveling to level tie lines and full leveling to level survey lines. The statistical leveling method corrected the SL/TL intersection errors that follow a specific pattern or trend. Through the error channel, an algorithm calculated a least-squares trend line and derived a trend error curve, which was then added to the channel to be leveled. The second component was full leveling. This adjusted the magnetic value of the survey lines so that all lines matched the trended tie lines at each intersection point.

Following statistical and full leveling, micro-leveling was applied to the corrected conventional leveled data. This iterative grid-based process removes low amplitude components of flight line noise that remain in the data after tie line and survey line leveling and results in fully leveled TMI data.

6.3.6 Reduction to Magnetic Pole

Reduced to Magnetic Pole (RTP) data were determined from the leveled Residual Magnetic Intensity (RMI) data. The RTP filter was applied in the Fourier domain and rotates the observed magnetic inclination and declination field to what the field would look like at the north magnetic pole, to allow observation of magnetic trends and patterns independent of magnetic inclination and declination. Reducing the dipolar nature of magnetic anomalies is useful for interpretation because peak RTP magnetic values can be related to the centre of magnetic rock bodies and asymmetries in the RTP imagery closely reflect true dips and plunges.

Inclination and declination were calculated by using July 6, 2022, the last day of the survey. The derived values were used in the following formula:

$$RTP\ (\theta) = \frac{[\sin(I) - I\ \cdot \cos(I) \cdot \cos(D-\theta)]^2}{[\sin^2(I_a) + \cos^2(I_a) \cdot \cos^2(D-\theta)] \cdot [\sin^2(I) + \cos^2(I) \cdot \cos^2(D-\theta)]}$$

where: I is geomagnetic inclination in ° from horizontal
D is geomagnetic declination in ° azimuth from magnetic north

I_a is the inclination for amplitude correction (never less than I). Default is ± 20°. If $|I_a|$ is specified to be less than$|I|$, it is set to I

6.3.7 Horizontal Gradient

Calculated Horizontal Gradient (CHG) is the magnitude of the total horizontal gradient. It is used to estimate contact locations of magnetic bodies at shallow depths, reveal anomaly texture, and highlight anomaly-pattern discontinuities.

If M is the magnetic field, then the CHG is calculated as:

$$\mathrm{CHG}(x,y) = \sqrt{\left(\frac{\partial M}{\partial x}\right)^2 + \left(\frac{\partial M}{\partial y}\right)^2}$$

where: $\frac{\partial M}{\partial x}$ is the E-W gradient
$\frac{\partial M}{\partial y}$ is the N-S gradient

6.3.8 Calculation of Vertical Gradient

Calculated Vertical Gradient (CVG) is the first order vertical derivative of the leveled Residual Magnetic Intensity (RMI) data. It is the vertical rate of change in the magnetic field per unit distance. The vertical gradient is used to enhance shorter wavelength signals; therefore, edges of magnetic anomalies are highlighted, and deep geologic sources in the data are suppressed.

The filter, L, used to produce the nth vertical derivative is described by:

$$L(r) = r^n$$

where: r is the radial component in the wavenumber domain

6.3.9 Analytic Signal

Analytic Signal (AS) is the magnitude of the total magnetic gradient in three axes, determined as the square root of the sum of the squares of the horizontal gradients and vertical gradient. Analytic signal is useful in locating the edges of magnetic source bodies.

If M is the magnetic field, then Analytic Signal (AS) is calculated as:

$$\mathrm{AS}(x,y,z) = \sqrt{\left(\frac{\partial M}{\partial x}\right)^2 + \left(\frac{\partial M}{\partial y}\right)^2 + \left(\frac{\partial M}{\partial z}\right)^2}$$

where: $\frac{\partial M}{\partial x}$ is the E-W gradient
$\frac{\partial M}{\partial y}$ is the N-S gradient
$\frac{\partial M}{\partial z}$ is the vertical gradient

6.4 Radiometric Processing

Radiometric surveys map gamma rays from the concentration of natural radioelements at or near the Earth surface; typically within 1 m of the surface. Before airborne radiometric data are processed, the spectrometer system is calibrated with the calibration pad test, cosmic flight test, and altitude correction and sensitivity test. Once calibration of the system was completed, radiometric data were processed by windowing the full 256 channel spectrum to create individual channels for U, Th, K, and total count (TC).

Potassium (^{40}K) is measured directly at 1.461 MeV and is reported as %K. Secular equilibrium in the decay chains of uranium (^{238}U determined from the radon daughter ^{214}Bi) and thorium (^{232}Th determined from ^{208}Tl) is assumed and the ground concentration results are reported as equivalent uranium (eU, ppm) and equivalent thorium (eTh, ppm). Total gamma count (TC) data (energy range from 0.40 to 2.81 MeV) is reported in dose rate (nGy/hr).

Radiometric processing generally followed the procedures provided by the International Atomic Energy Agency (IAEA) report 1363, *Guidelines for Radioelement Mapping using Gamma Ray Spectrometry Data*.

6.4.1 Calculation of Effective Height

Effective height (h_{ef}) in meters was determined using laser/radar altimeter, temperature, and pressure data, according to the formula below:

$$h_{ef} = h * \frac{273.15}{T + 273.15} * \frac{P}{1013.25}$$

where: h is measured laser/radar altitude in meters
T is measured air temperature in degrees Celsius
P is barometric pressure in millibars

6.4.2 Aircraft and Cosmic Background Corrections

Aircraft background and cosmic stripping corrections are applied to total gamma count and all three individual radioelements using the following formula:

$$C_{ac} = \mathrm{a}_c + b_c * Cos_f$$

where: C_{ac} is the background and cosmic corrected channel
a_c is the aircraft background for this channel
b_c is the cosmic stripping coefficient for this channel
Cos_f is the filtered cosmic channel

6.4.3 Radon Background Correction

Atmospheric radon can influence the gamma response of airborne radiometric data. The upward-looking detector provides directional sensitivity and the ability to discriminate between radiation from the atmosphere and radiation from the ground, to allow the removal of atmospheric radon effects from the downward-looking detectors.

Radon contribution to the uranium window of the "downward" uranium window is given by:

$$U_r = \frac{u - a_1 U - a_2 T + a_2 b_t - b_u}{a_u - a_1 - a_2 a_t}$$

where: U_r is radon background in the "downward" U window
u is count rate in the "upward" U window
U is count rate in the "downward" U window
T is count rate in the "downward" Th window
a_1, a_2, a_u, a_t, b_u, and b_t are constants derived by calibration

6.4.4 Compton Stripping

Spectral overlap corrections are applied to potassium, uranium, and thorium as part of the Compton stripping process. This is done by using the stripping ratios that have been calculated for the spectrometer by prior calibration.

For each of the stripping ratios α, β, and γ, height corrections at STP are made by using the following formulas:

$$\alpha_h = \alpha + h_{ef} * 0.00049$$

$$\beta_h = \beta + h_{ef} * 0.00065$$

$$\gamma_h = \gamma + h_{ef} * 0.00069$$

where: α, β, and γ are the Compton stripping coefficients
α_h, β_h, and γ_h are the height-corrected Compton stripping coefficients
h_{ef} is the effective height above ground in metres at STP

Stripping corrections are then carried out using the following formulas:

$$Th_c = Th_{bc}(1 - g\beta_h) + U_{bc}(b\gamma_h - a) + K_{bc}(ag - b)/A$$

$$U_c = Th_{bc}(g\beta_h - \alpha_h) + U_{bc}(1 - b\beta_h) + K_{bc}(b\alpha_h - g)/A$$

$$K_c = [Th_{bc}(\alpha_h\gamma_h - \beta_h) + U_{bc}(a\beta_h - \gamma_h) + K_{bc}(1 - a\alpha_h)]/A$$

where: U_c, Th_c, and K_c are stripping-corrected uranium, thorium, and potassium
α_h, β_h, and γ_h are height-corrected Compton stripping coefficients
U_{bc}, Th_{bc}, and K_{bc} are background corrected uranium, thorium, and potassium
a is the spectral ratio Th/U
b is the spectral ratio Th/K
g is the spectral ratio U/K
$A = 1 - g\gamma_h - (\alpha_h - g\beta_h) - b(\beta_h - \alpha_h\gamma_h)$ is the backscatter correction

6.4.5 Attenuation Corrections

Total count, potassium, uranium, and thorium data are then corrected to a nominal survey altitude (corrected to remove vegetation clutter from radar/laser altimeter data); in this case the nominal survey height was 50 m AGL. This is done according to the equation:

$$C_a = C * e^{\mu(h_{ef} - h_0)}$$

where: C_a is the output altitude-corrected channel
C is the input channel
μ is the attenuation correction for that channel
h_{ef} is the effective altitude
h_0 is the nominal survey altitude used as datum

6.4.6 Conversion to Apparent Radioelement Concentrations

With all corrections applied to the radiometric data, the final step is to convert the corrected potassium (^{40}K), uranium (from ^{214}Bi), and thorium (from ^{212}Tl) to apparent radioelement concentrations using the following formula:

$$eE = C_{cor}/S$$

where: eE is the element concentration of K (%) and equivalent element concentrations of U (ppm) & Th (ppm)
S is the experimentally determined sensitivity
C_{cor} is the fully corrected channel

Conversion of total count to natural exposure rate (Grasty et al, 1984) is determined by using the following formula:

$$\text{Natural Exposure} = [(1.505 * K) + (0.625 * eU) + (0.31 * eTh)]$$

where: Natural Exposure is in µR/hr
K is the concentration of potassium (%)
eU is the equivalent concentration of uranium (ppm)
eTh is the equivalent concentration of thorium (ppm)

6.4.7 Radiometric Ratios

Common radiometric ratios (U/Th, Th/K, U/K, and their inverses) were calculated using the guidelines of the IAEA. Due to statistical uncertainties in the individual radioelement measurements, care was taken during ratio calculation in order to obtain statistically significant values. The following guidelines were used to determine the ratios:

1. For each concentration, the lowest corrected count rate is determined.
2. Element concentrations of adjacent points on either side of each data point are summed until they exceed a pre-determined threshold value.
3. The ratios are calculated using the accumulated sums.

With these guidelines, errors associated with the calculated ratios are minimized and comparable for all data points.

6.4.8 Ternary Radioelement Image Map

Ternary images are a graphic representation of the relative proportion of the radioelement concentrations of %K, eTh, and eU components in proportion to the respective colours blue (cyan), red (magenta), and yellow. Since each distinct colour is used to represent each ternary ratio on the map, zones with similar ratios will be represented by a unique colour. This distinct relationship between colour and ternary ratio allows the map to show surficial radioelement concentration and distribution. Dark and light colours indicate high and low values for all three radionuclides, respectively. Areas of low radioactivity, and consequently low signal to noise ratios, can be masked and are shaded in white. Because the ternary image is a three-way ratio, topographic and physiographic effects are suppressed and a visualization of the relative concentrations of the

individual radioelements are presented to help discriminate between different zones of lithology and alteration.

7.0 Deliverables

Tosh survey data are presented as digital databases, grids, maps, and a logistics report.

7.1 Digital Data

Digital files have been provided in three formats:

- GDB file for use in Geosoft Oasis Montaj,
- XYZ file,
- CSV Excel comma separated file.

Full descriptions of the digital data and contents are included in Appendix D.

7.1.1 Grids

Digital data were represented as grids as listed below:

- Digital Terrain Model (DTM)
- Total Magnetic Intensity (TMI)
- Residual Magnetic Intensity (RMI) – removal of IGRF from TMI
- Reduced to Magnetic Pole (RTP) – reduced to magnetic pole of RMI
- Calculated Horizontal Gradient (CHG) – total magnitude of the horizontal gradients of RMI
- Calculated Vertical Gradient (CVG) – first order vertical derivative of RMI
- Analytic Signal (AS) – total gradient of RMI
- Potassium – Percentage (%K)
- Thorium – Equivalent Concentration (eTh)
- Uranium – Equivalent Concentration (eU)
- Total Count (TC)
- Total Count – Exposure Rate (TCexp)
- Potassium over Thorium Ratio (%K/eTh)
- Potassium over Uranium Ratio (%K/eU)
- Uranium over Thorium Ratio (eU/eTh)
- Uranium over Potassium Ratio (eU/%K)
- Thorium over Potassium Ratio (eTh/%K)
- Thorium over Uranium Ratio (eTh/eU)
- Ternary Image (TI)

Digital magnetic and radiometric data were gridded and displayed using the following Geosoft parameters:

- Gridding method: minimum curvature
- Grid cell size: 25 m
- Low-pass desampling factor: 2
- Tolerance: 0.001
- % pass tolerance: 99.99
- Maximum iterations: 100
- Shading effect: sun inclination at 45° and declination at 045°

Descriptions of colour scales are presented in Appendix D.

7.2 KMZ

Gridded digital data were exported into .KMZ files which can be displayed using Google Earth. The grids can be draped onto topography and rendered to provide a 3D view.

7.3 Maps

The following digital map products were prepared for Tosh:

Overview Maps (colour images with elevation contour lines):

- Actual flight lines, with topographic features
- DTM

Magnetic Maps (colour images with elevation contour lines):

- TMI, with topographic features and actual flight lines
- TMI
- RMI
- RTP
- CHG
- CVG
- AS

Radiometric Maps (colour images with elevation contour lines):

- %K – Percentage
- eTh – Equivalent Concentration
- eU – Equivalent Concentration
- TC

- TCexp – Exposure Rate
- %K/eTh Ratio
- %K/eU Ratio
- eTh/eU Ratio
- Ternary Image

All survey maps were prepared in WGS 84 in UTM Zone 7N.

7.4 Report

A .PDF copy of the logistics report is included along with digital data and maps. The report provides information on acquisition, processing, and presentation of the Tosh survey data.

8.0 Conclusions and Recommendations

The Tosh survey collected 913 line km of high resolution magnetic and radiometric data over one survey block. The data have been processed and plotted on maps as a representation of the features of the survey area.

When magnetic and radiometric data are integrated into a single-pass airborne survey, they provide complementary information that serves as a durable geophysical/geochemical framework. Therefore, the geophysical data will be useful in mapping lithology, structure, and alteration, which will benefit mineral exploration initiatives and geological studies.

Geophysical data processing, particularly leveling and data interpolation routines, tend to smooth the original data so that resolution is reduced. In addition, gridding algorithms are not always able to properly calculate grids where flight height between adjacent flight lines varied due to cultural obstacles or steep terrain, where geological structures are acute to flight lines, where line spacing exceeds the size of the causative anomaly, or near grid margins as in "edge effects." Therefore, subtle geophysical features observed near survey margins or in gridded and derivative-enhanced products must be evaluated with discretion.

The airborne geophysical data were acquired to map geophysical characteristics of the survey area, which are in turn related to the distribution of magnetic minerals and radioactive elements in the Earth. Magnetic patterns correspond to the concentration and distribution of magnetite and other magnetic minerals in Earth's subsurface. Radiometric data are influenced by topographic features and surficial effects, and ratios can be used to evaluate the near-surface radioelement geochemistry of the survey area.

Geophysical data are rarely a direct indication of mineral deposits and therefore interpretation and careful integration with existing and new geological, geochemical, and other geophysical data are recommended to maximize value from the survey investment.

Respectfully submitted,
Precision GeoSurveys Inc.

Jen D. Hanlon, M.Sc., P.Geo.
August 2022

Appendix A

Polygon Coordinates

Tosh Survey Block – WGS 84 Zone 7N

Latitude (deg N)	Longitude (deg W)	Easting (m)	Northing (m)
61.85489	139.54148	576752	6858876
61.87377	139.48311	579774	6861050
61.83363	139.42497	582939	6856651
61.83222	139.42933	582714	6856489
61.82261	139.41531	583478	6855437
61.78996	139.36691	586119	6851864
61.80966	139.30729	589205	6854138
61.76826	139.24635	592540	6849613
61.74861	139.30409	589551	6847344
61.76944	139.33398	587913	6849622
61.74378	139.40977	583984	6846665
61.80915	139.50381	578851	6853827
61.81567	139.48437	579859	6854577

Appendix B

Equipment Specifications

- GEM GSM-19T Proton Precession Magnetometer (Magnetic Base Station)
- Hemisphere R330 GPS Receiver
- Opti-Logic RS800 Rangefinder Laser Altimeter
- Scintrex CS-3 Magnetometer
- Billingsley TFM100G2 Ultra Miniature Triaxial Fluxgate Magnetometer
- Setra Model 276 Barometer
- Rotronic HygroClip HC-S3 Relative Humidity and Temperature Probe
- Nuvia Dynamics Advanced Gamma-Ray Spectrometer (AGRS-2)
- Nuvia Dynamics IMPAC data recorder system (for navigation and geophysical data acquisition)

GEM GSM-19T Proton Precession Magnetometer (Magnetic Base Station)

Sensitivity	0.15 nT @ 1 Hz
Resolution	0.01 nT (gamma), magnetic field and gradient
Absolute Accuracy	±0.2 nT @ 1 Hz
Operating Range	20,000 nT to 120,000 nT
Gradient Tolerance	Over 7,000 nT/m
Operating Ranges	Temperature: -40°C to +50°C Battery Voltage: 10.0 V minimum to 15 V maximum Humidity: up to 90% relative, non-condensing
Storage Temperature	-50°C to +50°C
Dimensions	Console: 223 x 69 x 40 mm Sensor Staff: 4 x 450 mm sections Sensor: 170 x 71 mm dia. Weight: console 2.1 kg, sensor and staff assembly 2.2 kg
Integrated GPS	Yes

Hemisphere R330 GPS Receiver

GPS Sensor	Receiver Type	L1 and L2 RTK with carrier phase	
	Channels	12 L1CA GPS 12 L1P GPS 12 L2P GPS 12 L2C GPS 12 L1 GLONASS (with subscription code) 12 L2 GLONASS (with subscription code) 3 SBAS or 3 additional L1CA GPS	
	Update Rate	10 Hz standard, 20 Hz available	
	Cold Start Time	<60 s	
	Warm Start Time 1	30 s (valid ephemeris)	
	Warm Start Time 2	30 s (almanac and RTC)	
	Hot Start Time	10 s typical (valid ephemeris and RTC)	
	Reacquisition	<1 s	
	Differential Options	SBAS, Autonomous, External RTCM, RTK, OmniSTAR (HP/XP)	
Horizontal Accuracy		RMS (67%)	2DRMS (95%)
	RTK [1, 2]	10 mm + 1 ppm	20 mm + 2 ppm
	OmniSTAR HP [1, 3]	0.1 m	0.2 m
	SBAS (WAAS) [1]	0.3 m	0.6 m
	Autonomous, no SA [1]	1.2 m	2.5 m
L-Band Sensor	Channel	Single channel	
	Frequency Range	1530 MHz to 1560 MHz	
	Satellite Selection	Manual or Automatic (based on location)	
	Startup and Satellite Reacquisition Time	15 seconds typical	
Communications	Serial Ports	2 full duplex RS232	
	Baud Rates	4800 – 115200	
	USB Ports	1 Communications, 1 Flash Drive data storage	
	Correction I/O Protocol	Hemisphere GPS proprietary, RTCM v2.3 (DGPS), RTCM v3 (RTK), CMR, CMR+NMEA 0183, Hemisphere GPS binary	
	Timing Output	1 PPS (HCMOS, active high, rising edge sync, 10 kΩ, 10 pF load)	
	Event Marker Input	HCMOS, active low, falling edge sync, 10 kΩ	
Environmental	Operating Temperature	-40°C to +70°C	
	Storage Temperature	-40°C to +85°C	
	Humidity	95% non-condensing	
Power GPS Sensor	Input Voltage Range	8 to 36 VDC	
	Consumption, RTK	<3.5 W (0.30 A @ 12 VDC typical)	
	Consumption, OmniSTAR	<4.3 W (0.36 A @ 12 VDC typical)	

[1]Depends on multipath environment, number of satellites in view, satellite geometry and ionospheric activity.
[2] Depends also on baseline length.
[3] Requires a subscription from OmniSTAR.

Opti-Logic RS800 Rangefinder Laser Altimeter

Accuracy	±1 m on 1x1 m^2 diffuse target with 50% reflectivity, up to 700 m
Resolution	0.2 m
Communication Protocol	RS232-8, N, 1 ASCII characters
Baud Rate	19200
Data Raw Counts	~200 Hz
Data Calibrated Range	~10 Hz
Data Rate	~200 Hz raw counts for un-calibrated operation; ~10 Hz for calibrated operation (averaging algorithm seeks 8 good readings)
Calibrated Range Units	Feet, Meters, Yards
Laser	Class I (eye-safe), 905 nm ± 10 nm
Power	7 - 9 VDC conditioned required, current draw at full power (~ 1.8 W)
Laser Wavelength	RS100 905 nm ± 10 nm
Laser Divergence	Vertical axis – 3.5 mrad half-angle divergence; Horizontal axis – 1 mrad half-angle divergence; (approximate beam "footprint" at 100 m is 35 cm x 5 cm)
Dimensions	32 x 78 x 84 mm (lens face cross section is 32 x 78 mm)
Weight	<227 g (8 oz)
Casing	RS100/RS400/RS800 units are supplied as OEM modules consisting of an open chassis containing optics and circuit boards. Custom housings can be designed and built on request.

Scintrex CS-3 Magnetometer

Operating Principal	Self-oscillating split-beam Cesium Vapor (non-radioactive ^{133}Cs)
Operating Range	15,000 nT to 105,000 nT
Gradient Tolerance	40,000 nT/m
Operating Zones	15° to 75° and 105° to 165°
Hemisphere Switching	a) Automatic b) Electronic control actuated by the control voltage levels (TTL/CMOS) c) Manual
Sensitivity	0.0006 nT / √Hz rms
Noise Envelope	Typically 0.002 nT peak to peak, 0.1 to 1 Hz bandwidth
Heading Error	±0.20 nT (inside the optical axis to the field direction angle range 15° to 75° and 105° to 165°)
Absolute Accuracy	<2.5 nT throughout range
Output	a) Continuous signal at the Larmor frequency which is proportional to the magnetic field (proportionality constant 3.49857 Hz/nT) sine wave signal amplitude modulated on the power supply voltage b) Square wave signal at the I/O connector, TTL/CMOS compatible
Information Bandwidth	Only limited by the magnetometer processor used
Sensor Head	Diameter: 63 mm (2.5”) Length: 160 mm (6.3”) Weight: 1.15 kg (2.6 lb)
Sensor Electronics	Diameter: 63 mm (2.5”) Length: 350 mm (13.8”) Weight: 1.5 kg (3.3 lb)
Cable, Sensor to Sensor Electronics	3 m (9’ 8”), lengths up to 5 m (16’ 4”) available
Operating Temperature	-40°C to +50°C
Humidity	Up to 100%, splash proof
Supply Power	24 to 35 VDC
Supply Current	Approx. 1.5 A at start up, decreasing to 0.5 A at 20°C
Power Up Time	Less than 15 minutes at -30°C

Billingsley TFM100G2 Ultra Miniature Triaxial Fluxgate Magnetometer

Axial Alignment	Orthogonality better than ±1°
Input Voltage Options	15 to 34 VDC @ 30 mA
Field Measurement Range Options	±100 µT = ±10 V
Accuracy	±0.75% of full scale (0.5% typical)
Linearity	±0.015% of full scale
Sensitivity	100 µV/nT
Scale Factor Temperature Shift	0.007% full scale/°C
Noise	≤12 pT rms/√Hz @ 1 Hz
Output Ripple	3 mV peak to peak @ 2nd harmonic
Analog Output at Zero Field	±0.025 V
Zero Shift with Temperature	±0.6 nT/°C
Susceptibility to Perming	±8 nT shift with ± 5 Gs applied
Output Impedance	332 Ω ± 5%
Frequency Response	3 dB @ >500 Hz (to >4 kHz wide band)
Over Load Recovery	±5 Gs slew <2 ms
Random Vibration	>20 G rms 20 Hz to 2 kHz
Temperature Range	-55°C to +85°C
Acceleration	>60 G
Weight	100 g
Size	3.51 cm x 3.23 cm x 8.26 cm
Connector	Chassis mounted 9 pin male "D" type

Setra Model 276 Barometer

Performance	Accuracy RSS[1] (at constant temp)	±0.25% FS[2]
	Non-Linearity (BSFL)	±0.22% FS
	Hysteresis	0.05% FS
	Non-Repeatability	0.05% FS
	Thermal Effects[3]	Compensated range: 0°C to +55°C (+30°F to +130°F) Zero shift (over compensated range): 1% FS Span shift (over compensated range): 1% FS
	Resolution	Infinite, limited only by output noise level (0.0005% FS)
	Time Constant	10 msecs to reach 90% final output with step function pressure input
	Long Term Stability	0.25% FS / 6 months
Environmental	Temperature	Operating[4]: -18°C to +79°C (0°F to +175°F) Storage: -55°C to +121°C (-65°F to +250°F)
	Vibration	2 g from 5 Hz to 500 Hz
	Shock	50 g (Operating, 1/2 sine 10 ms)
	Acceleration	10 g
Electrical	Circuit	3-Wire[5] (Exc, Out, Com)
	Power Consumption	0.20 W (24 VDC)
	Output Impedance	5 Ω
	Output Noise	<200 µV RMS (0 to 100 Hz)

[1] RSS of non-linearity, hysteresis, and non-repeatability.
[2] FS = 300 mb for 800 – 1100 mb range; 500 for 600 – 1100 mb range; and 20 PSI for 0 to 20 PSIA.
[3] Units calibrated at nominal 70°F. Maximum thermal error computed from this datum.
[4] Operating temperature limits of the electronics only. Pressure media temperatures may be considerable higher or lower.
[5] The separate leads for +EXC, -EXC, +Out, -Out are commoned internally. The shield is connected to the case. For best performance, either the -Exc or -Out should be connected to the case. Unit is calibrated at the factory with -Exc connected to the case. The insulation resistance between all signal leads are tied together and case ground is 100 Ω minimum at 25 VDC.

Rotronic HygroClip HC-S3 Relative Humidity and Temperature Probe

Relative Humidity	Operating Range	0 to 100% RH
	Accuracy at 23°C	±1.5% RH
	Output	0 – 1 VDC
	Typical Long-Term Stability	Better than ±1% RH per year
Temperature	Measurement Range	-40°C to +60°C
	Temperature Accuracy	-30°C to +60°C ±0.2°C -50°C to +60°C ±0.6°C (worst case)
	Output	0 – 1 VDC
Power	Supply Voltage	3.5 to 50 VDC (typically powered by data logger's 12 VDC supply)
	Current Consumption	<4 mA
Dimensions	Diameter	1.53 cm (0.60")
	Length	16.8 cm (6.6")
	Housing Material	Polycarbonate

Nuvia Dynamics Advanced Gamma-Ray Spectrometer (AGRS-2)

Crystal Volume	Two 4.2 L NaI(Tl) synthetic downward-looking crystals. Total volume of 8.4 L
Resolution	256/512/1024 channels
Data Handling	Individual detector processing and calibration
Energy Resolution	< 9% (@ 662 keV)
Differential Non-linearity	< 0.1%
Integral Non-linearity	< 0.01%
Gain Stabilization	Automatic multi-peak on natural radioisotopes
Calibration	Automatic using natural background radiation
Dynamic Input Range	250,000 cps (counts/sec) per detector
Baseline Restoration	Digital Individual Pulse Baseline Restoration (IPBR). The baseline is established for each individual pulse for maximum pulse height accuracy
Sampling Rate	0.1 – 10 secs user defined
Pulse Shaping	Digital Pulse Shaping
Power	9 to 40 VDC, 15 W
Detector Power	3 W per detector
Operating Temperature	-20°C up to +50°C
Upward Shielding	RayShield® non-radioactive shielding on downward-looking crystals
Spectra	20 keV to 3 MeV (plus cosmic)
System Stabilization	Cold start-up: less than 40 secs on the ground
GPS Connectivity	Time and position synchronization; additional add-on
Weight	~115 kg

Nuvia Dynamics IMPAC data recorder system

(for navigation and geophysical data acquisition)

Functions	Integrated Multi-Parameter Airborne Console (IMPAC) with integrated dual Global Positioning System Receiver (GPS) and all necessary navigation guidance software. Inputs for geophysical sensors - portable gamma ray spectrometer GRS-10/AGRS, MMS4/MMS8 Magnetometer, Herz Totem-2A EM, A/D converter, temperature/humidity probe, barometric pressure probe, and laser/radar altimeter. Output for the multi-parameter PGU (Pilot Guidance Unit)
Display	Monitor display 600 x 800 pixels; customized keypad and operator keyboard. Multi-screen options for real-time viewing of all data inputs, fiducial points, flight line tracking, and GPS channels by operator
Navigation	Pilot/operator navigation guidance. Software supports preplanned survey flight plan, along survey lines, way-points, preplanned drape profile surfaces
Data Sampling	Sensor dependent
Data Synchronization	Synchronized to GPS position. Supports dual GPS
Data File	PEI Binary data format
Storage	80 GB
Software	DataView: Allows fast data verification and conversion of PEI binary data to Geosoft GBN or ASCII formats MAGConv: For survey preparation, calibration and conversion of maps, and survey plot after data acquisition MAGComp: For calculation of magnetic compensation coefficients AGRS/GRS10 Calibration: High voltage adjustment, linearity correction coefficients calculation, and communication test support AGIS: Real time data acquisition and navigation system. Displays chart/spectrum view in real-time for fast data Quality Control (QC)
Electrical	Multiple ethernet connections, RS232 serial ports, USB ports, and 16-bit differential analog input channels. It can support up to 4 magnetometer sensors
Power Requirement	24 VDC

Appendix C

Radiometric Correction Coefficients

Radiometric Correction Coefficients:

Cosmic Correction Coefficients		
	Cosmic Stripping	**Aircraft Background**
TC	0.52955	31.043
K	0.04395	3.8530
U	0.04740	1.9192
Th	0.06830	0.4077

Altitude Attenuation Coefficients	
TC	-0.005
K	-0.007
U	-0.004
Th	-0.004

Compton Stripping	
Alpha	0.3191
Beta	0.4465
Gamma	0.8521
GrastyBackscatter_a	0.0518
GrastyBackscatter_b	0.0058
GrastyBackscatter_g	0.0024

Sensitivities	
TC	23.00
K	76.39
U	6.435
Th	3.454

Appendix D

Digital File Descriptions

- Magnetic Database
- Radiometric Database
- Geosoft Grids
- Maps

Magnetic Database:

Abbreviations used in the GDB/XYZ/CSV files are listed below:

CHANNEL	UNITS	DESCRIPTION
X_WGS84	m	UTM Easting – WGS84 Zone 7N
Y_WGS84	m	UTM Northing – WGS84 Zone 7N
Lat_deg	Decimal degree	Latitude – WGS84
Lon_deg	Decimal degree	Longitude – WGS84
Date	yyyy/mm/dd	Dates of the survey flight(s) – Local
FLT		Flight number(s)
LineNo		Line numbers
STL		Number of satellite(s)
GPSfix		1 = non-differential 2 = WAAS/SBAS differential
Heading	degree	Heading of the aircraft
GPStime	HH:MM:SS	GPS time (UTC)
Geos_m	m	Geoidal separation
XTE_m	m	Cross track error
Galt	m	GPS height – WGS84 Zone 7N (ASL)
Lalt	m	Laser altimeter readings (AGL)
DTM	m	Digital Terrain Model
Sample_Density	m	Horizontal distance in meters between adjacent measurement locations; sample frequency is 20 Hz
Speed_km_hr	km/hr	Ground speed of aircraft in km/hr
basemag	nT	Base station temporal variation data
IGRF	nT	International Geomagnetic Reference Field, IGRF-13
Declin	Decimal degree	Calculated declination of magnetic field
Inclin	Decimal degree	Calculated inclination of magnetic field
XFg_Step	step	X - fluxgate
YFg_Step	step	Y - fluxgate
ZFg_Step	step	Z - fluxgate
Mag_Head	nT	Diurnal, lag, and heading corrected
TMI	nT	Total Magnetic Intensity
RMI	nT	Residual Magnetic Intensity

Radiometric Database:

Abbreviations used in the GDB/XYZ/CSV files listed below:

CHANNEL	UNITS	DESCRIPTION
X_WGS84	m	UTM Easting – WGS84 Zone 7N
Y_WGS84	m	UTM Northing – WGS84 Zone 7N
Lat_deg	Decimal degree	Latitude – WGS84
Lon_deg	Decimal degree	Longitude – WGS84
Date	yyyy/mm/dd	Date of the survey flight(s) – Local
FLT		Flight Line numbers
LineNo		Line numbers
STL		Number of satellite(s)
GPStime	HH:MM:SS	GPS time (UTC)
Geos_m	m	Geoidal separation
GPSFix		1 = non-differential 2 = WAAS/SBAS differential
Heading	degree	Heading of the aircraft
XTE_m	m	Cross track error
Galt	m	GPS height – WGS84 Zone 7N (ASL)
Lalt	m	Laser altimeter height (AGL)
DTM	m	Digital Terrain Model
Sample_Density	m	Horizontal distance in metres between adjacent measurement locations; sample frequency is 20 Hz
Speed_km_hr	km/hr	Ground speed of aircraft in km/hr
BaroSTP_kPa	kPa	Barometric altitude (pressure and temperature corrected)
Temp_degC	°C	Air temperature
COSFILT	counts/sec	Spectrometer – Filtered Cosmic
Kcor	%	Concentration in Percentage - Potassium
Thcor	ppm	Equivalent Concentration - Thorium
Ucor	ppm	Equivalent Concentration - Uranium
TCcor	nGy/hour	Total Count
TCexp	µR/hour	Exposure Rate
KThratio		Spectrometer –%K/eTh ratio
KUratio		Spectrometer –%K/eU ratio
ThKratio		Spectrometer – eTh/%K ratio
ThUratio		Spectrometer – eTh/eU ratio
UKratio		Spectrometer – eU/%K ratio

Grids:

Tosh, WGS 84 Zone 7N, sun inclination at 45° and declination at 045°

File Name	Description	Cell Size (m)
22149_Tosh_DTM_25m.grd	Digital Terrain Model	25
22149_Tosh_TMI_25m.grd	Total Magnetic Intensity	25
22149_Tosh_RMI_25m.grd	Residual Magnetic Intensity	25
22149_Tosh_RTP_25m.grd	Reduced to Magnetic Pole of RMI	25
22149_Tosh_CHG_25m.grd	Calculated Horizontal Gradient	25
22149_Tosh_CVG_25m.grd	Calculated Vertical Gradient of RMI	25
22149_Tosh_AS_25m.grd	Analytic Signal of RMI	25
22149_Tosh_K_25m.grd	Potassium (%K) – in percentage	25
22149_Tosh_eTh_25m.grd	Thorium (eTh) – equivalent concentration	25
22149_Tosh_eU_25m.grd	Uranium (eU) – equivalent concentration	25
22149_Tosh_TC_25m.grd	Total Count (TC)	25
22149_Tosh_TCexp_25m.grd	Total Count (TCexp) – exposure rate	25
22149_Tosh_KThRatio_25m.grd	Potassium over Thorium ratio (%K/eTh)	25
22149_Tosh_KURatio_25m.grd	Potassium over Uranium ratio (%K/eU)	25
22149_Tosh_UThRatio_25m.grd	Uranium over Thorium ratio (eU/eTh)	25
22149_Tosh_UKRatio_25m.grd	Uranium over Potassium ratio (eU/%K)	25
22149_Tosh_ThKRatio_25m.grd	Thorium over Potassium ratio (eTh/%K)	25
22149_Tosh_ThURatio_25m.grd	Thorium over Uranium ratio (eTh/eU)	25

Maps:

Tosh, WGS 84 Zone 7N, sun inclination at 45° and declination at 045°
(JPEG, PDF, and georeferenced PDF)

Plate Num	Plate Name	File Name	Description	Cell Size (m)	Colour Scale	Colour Shade
1	FL	22149_Tosh_ActualFlightLines	Plotted actual flown flight lines	NA	NA	NA
2	DTM	22149_Tosh_DTM_25m	Digital Terrain Model	25	Linear	NA
3	TMI_wFL	22149_Tosh_TMI_wFL_25m	Total Magnetic Intensity with actual flown flight lines	25	Histogram -equalized	RGB
4	TMI	22149_Tosh_TMI_25m	Total Magnetic Intensity	25	Histogram -equalized	RGB
5	RMI	22149_Tosh_RMI_25m	Residual Magnetic Intensity	25	Histogram -equalized	RGB
6	RTP	22149_Tosh_RTP_25m	Reduced to Magnetic Pole of RMI	25	Histogram -equalized	RGB
7	CHG	22149_Tosh_CHG_25m	Calculated Horizontal Gradient of RMI	25	Histogram -equalized	Wet-look
8	CVG	22149_Tosh_CVG_25m	Calculated Vertical Gradient of RMI	25	Histogram -equalized	Wet-look
9	AS	22149_Tosh_AS_25m	Analytic Signal of RMI	25	Histogram -equalized	Wet-look
10	%K	22149_Tosh_K_25m	Potassium (%K) – in percentage	25	Histogram -equalized	RGB
11	eTh	22149_Tosh_eTh_25m	Thorium (eTh) – equivalent concentration	25	Histogram -equalized	RGB
12	eU	22149_Tosh_eU_25m	Uranium (eU) – equivalent concentration	25	Histogram -equalized	RGB
13	TC	22149_Tosh_TC_25m	Total Count (TC)	25	Histogram -equalized	RGB
14	TCexp	22149_Tosh_TCexp_25m	Total Count (TCexp) – exposure rate	25	Histogram -equalized	RGB
15	%K/eTh	22149_Tosh_KThRatio_25m	Potassium over Thorium ratio (%K/eTh)	25	Histogram -equalized	RGB
16	%K/eU	22149_Tosh_KURatio_25m	Potassium over Uranium ratio (%K/eU)	25	Histogram -equalized	RGB
17	eTh/eU	22149_Tosh_ThURatio_25m	Thorium over Uranium ratio (eTh/eU)	25	Histogram -equalized	RGB
18	TI	22149_Tosh_TernaryImage_25m	Ternary ratio of all three elements (%K, eTh, eU)	25	Histogram -equalized	RGB inverted

*Grids displayed on the maps are exported as GeoTIFFs (.tiff) and KMZs.

Plates

Tosh Survey Block

- Plate 1: Tosh – Actual Flight Lines (FL)
- Plate 2: Tosh – Digital Terrain Model (DTM)
- Plate 3: Tosh – Total Magnetic Intensity with Actual Flight Lines (TMI_wFL)
- Plate 4: Tosh – Total Magnetic Intensity (TMI)
- Plate 5: Tosh – Residual Magnetic Intensity (RMI)
- Plate 6: Tosh – Reduced to Magnetic Pole (RTP) of RMI
- Plate 7: Tosh – Calculated Horizontal Gradient (CHG) of RMI
- Plate 8: Tosh – Calculated Vertical Gradient (CVG) of RMI
- Plate 9: Tosh – Analytic Signal (AS) of RMI
- Plate 10: Tosh – Potassium - Percentage (%K)
- Plate 11: Tosh – Thorium - Equivalent Concentration (eTh)
- Plate 12: Tosh – Uranium - Equivalent Concentration (eU)
- Plate 13: Tosh – Total Count (TC)
- Plate 14: Tosh – Total Count - Exposure Rate (TCexp)
- Plate 15: Tosh – Potassium over Thorium Ratio (%K/eTh)
- Plate 16: Tosh – Potassium over Uranium Ratio (%K/eU)
- Plate 17: Tosh – Thorium over Uranium Ratio (eTh/eU)
- Plate 18: Tosh – Ternary Image (TI)